Rapid thermal equilibration in coarse-grained molecular dynamics

S. P. A. Gill
Department of Engineering, University of Leicester, University Road, Leicester LE1 7RH, United Kingdom

Z. Jia
Institute of Computational Mathematics, Chinese Academy of Sciences (CAS), Beijing 100080, China

B. Leimkuhler
Department of Mathematics, University of Leicester, University Road, Leicester LE1 7RH, United Kingdom

A. C. F. Cocks
Department of Engineering, University of Leicester, University Road, Leicester LE1 7RH, United Kingdom
(Received 27 May 2005; revised manuscript received 12 December 2005; published 23 May 2006)

Coarse-grained representations of matter are required for the investigation of material phenomena that occur simultaneously at different length and time scales. Multiple scales cause problems at finite temperature, where phonon reflection at interfaces separating different scales causes unphysical local heating in the region of the smallest (atomic) scale. A physical model is proposed, which effectively controls the temperature in coarse-grained regions while preserving correct dynamics in the atomistic region. This is achieved using a multiscale dynamic-stochastic heat bath. The validity of the model is demonstrated within the context of a coarse-grained one-dimensional Lennard-Jones chain.

DOI: 10.1103/PhysRevB.73.184304 PACS number(s): 65.40.De, 02.70.Ns, 02.70.Dh, 45.20.Jj

I. INTRODUCTION

The boundary conditions for molecular dynamics (MD) simulations in the condensed phase are a compromise between the correct representation of the far field and the minimization of the system size due to computational constraints. In recent years, concurrent multiscale methods have been developed for crystalline solids in which the far field is represented by a coarse-grained (CG) continuum constructed from finite elements.[1,2] The requirements of the CG far field depend on the nature of the simulation, generally either sampling or dynamics. If the purpose is the sampling of equilibrium quantities, then typically only slowly changing thermodynamical or statistical quantities are of interest, and inertial effects are small. Rapid changes occur in truly dynamic situations such as fast fracture.

Dynamical simulations are complicated by the reflection of high-frequency phonons from the interface between the atomistic (AR) and CG regions. This leads to energy trapping and localized heating.[2] In most cases, the CG region is only required to provide a (slowly evolving) statistically accurate (elastostatic) far-field representation. Correct transmission of phonons across the interface[1–3] is only necessary if the far boundaries can be seen during the simulation period [e.g. microelectromechanical systems (MEMS)], or there are two ARs that need to interact dynamically via the CG medium (e.g., two cracks). Here, we assume that the absorption of phonons at the interface is a sufficient requirement.

The ensemble is consequently canonical (constant temperature) as opposed to microcanonical (constant energy). Conventional thermostatting algorithms control the temperature via velocity rescaling, which corrupts the true dynamics. Liu *et al.*[4] have recently demonstrated that MD simulations of nanoindentation are very sensitive to global thermostatic control.

This paper aims to address the problem of phonon reflection, while preserving the correct dynamics in the atomistic region. We proceed in four stages. First, a finite-temperature CG representation of the body is developed and compared with atomistic results. The choice of an appropriate interface between the CG and AR is then explored. The performance of different local thermostatting algorithms is assessed in the context of correct sampling, and, finally, the more demanding requirements of dynamical simulation are considered.

II. THE COARSE-GRAINED SYSTEM

For the purpose of demonstration, we restrict the analysis to a one-dimensional (1D) chain of N atoms. Each atom, a, has mass m, position q_a, and momentum p_a where $a=1,\ldots,N$. Atoms interact via the pairwise potential $\phi(r)$, which is a function of separation r. The dynamics of the above system are described by the following Hamiltonian:

$$H(\boldsymbol{Q},\boldsymbol{P}) = \frac{\boldsymbol{P}^T\boldsymbol{M}^{-1}\boldsymbol{P}}{2} + V(\boldsymbol{Q}), \tag{1}$$

where $\boldsymbol{P}=\{p_a\}$, $\boldsymbol{Q}=\{q_a\}$, $\boldsymbol{M}=m\boldsymbol{I}$, $\boldsymbol{I}$ is the identity matrix and $V(\boldsymbol{Q})$ is the total potential energy.

A. The effective coarse-grained Hamiltonian

It is the objective of this paper to reduce the number of degrees of freedom of the fully atomistic model defined in (1) while preserving the dynamical and sampling properties of part or all of the system. Following the philosophy of the quasicontinuum method,[5,6] a reduced set of $n(<N)$ atoms are chosen to represent the system. In a 1D chain, these representative atoms form the ends of subchains of atoms. The behavior of the (slave) atoms within each subchain (or ele-

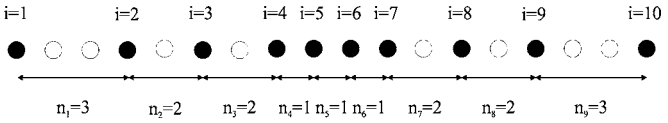

FIG. 1. Coarse-grained geometry of a 1D chain with ten representative atoms (●) and eight slave atoms (○).

ment) are inferred from the behavior of the representative atoms at each end. The representative atoms are given the indices $i=1,\ldots,n$, and each element i is bounded by representative atoms i and $i+1$. The level of coarse graining within an element is defined by n_i, the number of atoms associated with the element, such that element i contains n_i-1 slave atoms (representative atoms are shared between two elements). An example of the coarse-graining process is illustrated in Fig. 1 for $N=18$ and $n=10$. This is described by the set $\{3^1,2^2,1^3,2^2,3^1\}$.

Thus, the state of the system is characterized by the positions, $\boldsymbol{q}$, and momenta, $\boldsymbol{p}$, of the representative atoms. To retain correct sampling of these and related quantities, the artition function must remain constant[7]

$$Z=\frac{1}{h^N}\int_{\infty}^{\infty}\int_{\infty}^{\infty}\exp[-\beta H(\boldsymbol{Q},\boldsymbol{P})]d\boldsymbol{Q}d\boldsymbol{P}$$

$$=\frac{1}{h^n}\int_{\infty}^{\infty}\int_{\infty}^{\infty}\exp[-\beta H_{CG}(\boldsymbol{q},\boldsymbol{p})]d\boldsymbol{q}d\boldsymbol{p}, \qquad (2)$$

where h is the Planck constant, $\beta=1/k_BT$, k_B is the Boltzmann constant, and T is the absolute temperature. The resulting coarse-grained Hamiltonian is

$$H_{CG}(\boldsymbol{q},\boldsymbol{p})=\frac{\boldsymbol{p}^T\boldsymbol{m}^{-1}\boldsymbol{p}}{2}+V_{CG}(\boldsymbol{q},T), \qquad (3)$$

where the mass matrix $\boldsymbol{m}=m\boldsymbol{I}$ only contains the masses of the representative atoms. In fact, masses in the CG region are arbitrary as dynamics is only modeled in the AR. For consistency with other approaches,[7] we have utilized a lumped mass model (the mass of the slave atoms is also attributed to the representative atoms).

The CG potential $V_{CG}(\boldsymbol{q},T)$ can only be calculated analytically for a harmonic interatomic potential. Assuming only nearest-neighbor interactions with $\phi(r)=\frac{1}{2}k(r-r_0)^2$ gives

$$V_{CG}(\boldsymbol{q},T)=\frac{1}{2}\sum_{i=1}^{n-1}\frac{k}{n_i}(q_{i+1}-q_i-n_ir_0)^2$$

$$+k_BT\sum_{i=1}^{n-1}(n_i-1)\ln\left(\frac{\hbar\omega_i}{k_BT}\right), \qquad (4)$$

where the frequency $\omega_i=n_i^{1/[2(n_i-1)]}\sqrt{\frac{k}{m}}$. The first term on the rhs of (4) is the potential energy of the deformed lattice. The second term represents the vibrational energy of the slave atoms and is constant for a harmonic potential. Anharmonic effects such as thermal expansion only arise for nonlinear potentials. We make the approximation that (4) can be extended for a general potential such that the variant contribution is

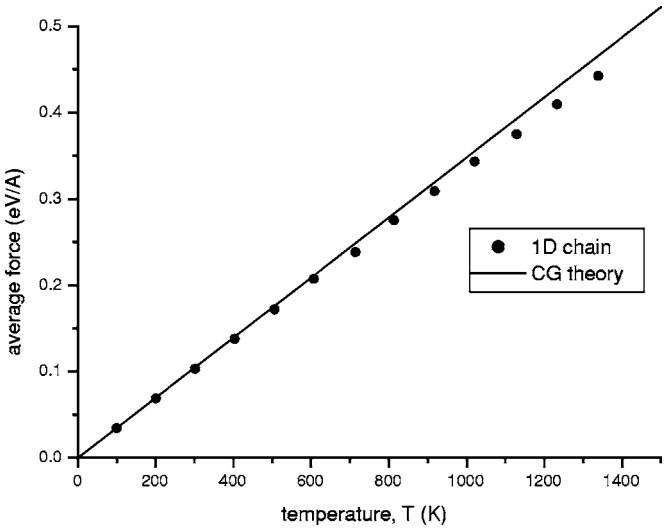

FIG. 2. Average thermal expansion force in a fully atomistic chain with predictions from the coarse-grained potential (5).

$$V_{CG}(\boldsymbol{q},T)=\sum_{i=1}^{n-1}n_i\phi(r_i)+\frac{1}{2}k_BT\sum_{i=1}^{n-1}(n_i-1)\ln\left(\left.\frac{\partial^2\phi}{\partial r^2}\right|_{r=r_i}\right), \qquad (5)$$

where $r_i=(q_{i+1}-q_i)/n_i$ is the mean interatomic spacing in element i. This is similar to the result of LeSar *et al.*[8] for high temperatures. Equation (5) reduces to the atomistic potential for no coarse graining (all $n_i=1$) as expected. Note that representative atoms only truly represent the time-averaged response of an atom (or group of atoms); their oscillation period and amplitude are not those of a normal atom.

B. Testing the coarse-grained potential

For illustration, the Lennard-Jones potential $\phi(r)=4\epsilon\left[\left(\frac{\sigma}{r}\right)^{12}-\left(\frac{\sigma}{r}\right)^{6}\right]$ is used. Only nearest-neighbor interactions are considered. In the simulations presented here, we took typical values of $\epsilon=0.6$ eV, $\sigma=2.5$ Å, and $m=10^{-25}$ kg. However, these results are general and the exact choice of parameters is not critical. The simulations are initialized by assigning representative atoms momenta from an appropriately weighted Gaussian distribution with zero net momentum. The ends of the chain are fixed so that the average lattice spacing is always the zero Kelvin lattice spacing, $r_0=\sqrt[6]{2}\sigma$.

For constrained thermal expansion, the average force acting between each atom is predicted to be $\lim_{n_i\to\infty}\left(-\frac{1}{n_i}\left.\frac{\partial V_{CG}}{\partial r}\right|_{r=r_0}\right)$ for a large, single ($n=2$) element. This is a linear function of temperature. Comparison with measurements from a 160-atom fully atomistic simulation in Fig. 2 shows a very small error at lower temperatures rising to only a small difference ($<3\%$) at 1000 °C.

It is worthwhile noting at this stage that the coarse-grained potential (5) is singular when $\frac{\partial^2\phi}{\partial r^2}=0$ (this occurs at $r=1.109r_0$). The singularity arises because the anharmonic potential (5) is approximated from the harmonic potential

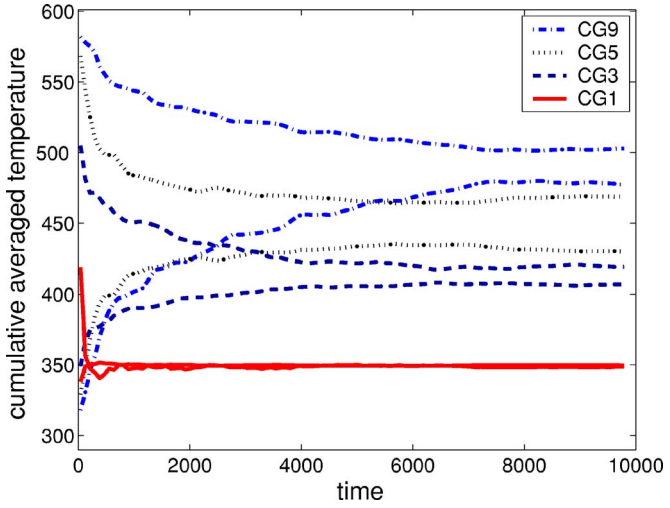

FIG. 3. (Color online) Redistribution of thermal energy between the atomistic region (AR), initially at 600 K, and the coarse-grained region (CG), initially at 300 K. The fully atomistic simulation (CG1) rapidly reaches an equilibrium temperature of 348 K. Any coarse graining drastically reduces the rate of convergence to the equilibrium. Increasing the level of coarse graining in the CG region from $n_i=3$ (CG3) up to $n_i=9$ (CG9) exacerbates the effect. Note that this is not a model of heat conduction. Thermal equilibrium is achieved when each degree of freedom (DOF) has the same average kinetic energy. Coarse graining reduces the DOF so the average kinetic energy (and equilibrium temperature) is higher. The time scales have been adjusted so that the results are directly comparable for the reduced temperature gradients.

(4). Numerical calculations using higher-order approximations remove the singularity but are computationally very expensive. Practically, as seen in Fig. 2, the mean atomic position is well approximated by the analytical expression (5). The region of the singularity is only sampled in a dynamic sense by infrequent large thermal fluctuations. This issue is addressed in the application of the numerical algorithms by using time-averaged values for some variables.

C. Thermal equilibrium of coarse-grained systems

The effect of coarse graining on the redistribution of thermal energy within the chain is now investigated. A chain of 1250 atoms is initiated far from thermal equilibrium, with the central 200 atoms at 600 K and the rest at 300 K. Figure 3 shows that this fully atomistic chain (CG1) rapidly reaches an equilibrium temperature of 348 K within a few hundred time units (one time unit is a single harmonic oscillation period). Now, the central 200 atoms are retained as the atomistic region (AR) and the rest form the coarse grained (CG) region. Figure 3 shows that any coarse graining drastically slows the convergence to equilibrium with the effect becoming more pronounced with increasing levels of coarse graining. The thermal energy separation between the regions arises due to the different length scales. High-frequency phonons in the AR are not supported in the CG region and can only cross the interface between them via the gradual process of nonlinear phonon interactions. The dramatic coarse-graining effects seen in Fig. 3 can be ameliorated (although not removed) by smoothing the transition from the AR to high levels of coarse graining via an interface (IF) region. For the rest of this paper, the chain will be configured as $\{9^{48},7^5,5^5,3^5,1^{18},1^{200},1^{18},3^5,5^5,7^5,9^{48}\}$. The two $\{9^{48}\}$ regions are denoted as CG9, the central $\{1^{200}\}$ region is denoted as AR, and the two intermediate regions of $\{7^5,5^5,3^5,1^{18}\}$ are denoted as IF.

III. NOSÉ AND NOSÉ-POINCARÉ THERMOSTATS

A common approach to temperature control is to apply a thermostat to the whole system. This can be done using the well-known Nosé Hamiltonian[9]

$$\mathcal{H}_{Nosé}(\boldsymbol{q},\tilde{\boldsymbol{p}},s,\pi)=\frac{\tilde{\boldsymbol{p}}^T\boldsymbol{m}^{-1}\tilde{\boldsymbol{p}}}{2s^2}+\frac{\pi^2}{2\mu}+V_{CG}(\boldsymbol{q},T)+gk_BT\ln s, \tag{6}$$

where s and π are conjugate position and momentum thermostatting variables, μ is a fictional thermal mass, and g is the number of degrees of freedom (including s). The virtual momenta $\tilde{\boldsymbol{p}}$ is related to the actual momenta by $\tilde{\boldsymbol{p}}=s\boldsymbol{p}$. In practice, the time scale must be reparametrized for numerical computation. A symplectic scheme with the reparametrization of time can be realized by the Nosé-Poincaré (NP) Hamiltonian[10] $\mathcal{H}_{NP}=s(\mathcal{H}_{Nosé}-\mathcal{H}_0)$ where $\mathcal{H}_0$ is the initial value of the Nosé Hamiltonian. (The use of symplectic NP-based schemes has stability advantages[10–12] compared to the more common Nosé-Hoover method.) Results are shown in Fig. 4(a) for $\mu=0.5$. The temperature approaches the desired value, but there is always a temperature separation between the scales. This demonstrates that applying a single NP thermostat to a system containing multiple length and time scales is not a particularly effective equilibration technique.

IV. PARTIAL THERMOSTATTING MOLECULAR DYNAMICS

Thermostatting the entire system is also undesirable from a modeling perspective as velocity rescaling can potentially corrupt the dynamics of the AR region. The partial thermostatting molecular dynamics (PTMD) technique proposed by Jia and Leimkuhler[13] addresses this problem. In this method, the set of representative atoms is divided into two sets, with positions $\boldsymbol{q}=\{\boldsymbol{q}_a,\boldsymbol{q}_b\}$, associated momenta $\boldsymbol{p}=\{\boldsymbol{p}_a,\boldsymbol{p}_b\}$, and masses $\boldsymbol{m}=\{\boldsymbol{m}_a,\boldsymbol{m}_b\}$ where a and b denote thermostatted and unthermostatted degrees of freedom, respectively. Applying a Nosé thermostat to set a gives the partial thermostatting Hamiltonian

$$\mathcal{H}^{PT}_{Nosé}=\frac{\tilde{\boldsymbol{p}}_a^T\boldsymbol{m}_a{}^{-1}\tilde{\boldsymbol{p}}_a}{2s^2}+\frac{\tilde{\boldsymbol{p}}_b^T\boldsymbol{m}_b{}^{-1}\tilde{\boldsymbol{p}}_b}{2}+\frac{\pi^2}{2\mu}+V_{CG}(\boldsymbol{q},T)+gk_BT\ln s. \tag{7}$$

A time transformation is applied to regularize the time variable for the thermostatted (a) variables.[13] The resulting system can be viewed as coupling Newtonian dynamics for the b variables with a Nosé-Poincaré style thermal reservoir. The PTMD model preserves volume and recovers the canonical

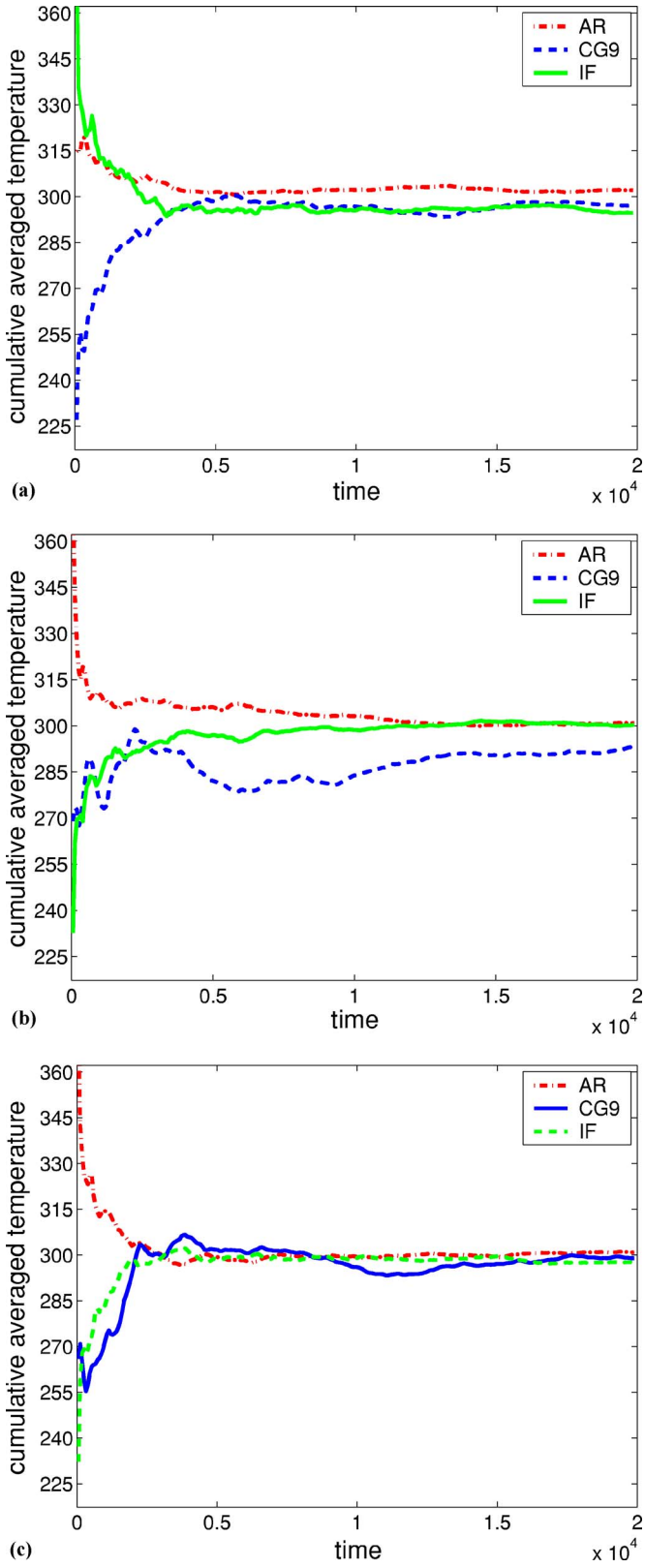

FIG. 4. (Color online) Comparison of different thermostatting techniques to the {CG9,IF,AR,IF,CG9} chain. The AR is initially at 600 K and the rest at 300 K. Results are for (a) NP to the whole chain, (b) NP to IF only, and (c) RMT to IF only, where the latter two are achieved using PTMD.

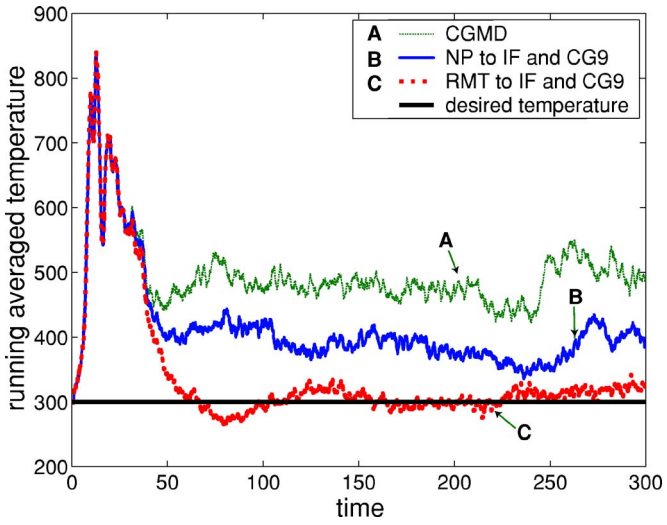

FIG. 5. (Color online) Running average of temperature in the AR for no thermostatting (CGMD), thermostatting with NP applied to IF and CG9, and thermostatting with RMT applied to IF and CG9. Only RMT absorbs the high-frequency phonons at the IF, and hence correctly regulates the temperature in the AR.

distribution.[13] This allows the temperature of any part of the chain to be directly regulated, forming an effective heat bath for the remainder of the system. The problem of Fig. 3 is now revisited. The temperature is initiated far from the thermal equilibrium, with the AR at 600 K and the rest (IF and CG9) thermostatted at 300 K using PTMD. The results are shown in Fig. 4(b). It is found that the PTMD thermostat provides a reasonable heat bath for the AR. However, the scale separation problem encountered in Fig. 4(a) still persists, and the equilibration time is increased.

Next, thermostatting a more demanding dynamic application is considered. The chain is initially equilibrated at 300 K, and then kinetic energy is injected into the AR from time $t=0$ to $t=20$ by forcing the central atom in the AR to oscillate with an amplitude of $0.03r_0$ and at 1.2 times harmonic oscillation frequency. This generates a succession of high-frequency traveling waves, which rapidly raise the temperature in the AR as shown in Fig. 5. The energy packet reaches the IF at $t=25$ and should have left the AR by $t=45$. Almost 50% of this energy is trapped in the AR if the simulation is unthermostatted [coarse-grained molecular dynamics (CGMD)]. Application of NP to IF and CG9 does not provide a good solution to this problem, because a single thermostat cannot respond rapidly to regions operating at different time scales resulting in phonon reflection at the AR/IF interface.

V. RECURSIVE MULTIPLE THERMOSTATS

Applying a single NP thermostat to a system containing multiple length and time scales is not a particularly effective equilibration technique. In practice, any thermostatting technique can be used within the PTMD algorithm. The multiscale thermostatting problem can be resolved within a Hamiltonian framework by use of the recursive multiple

thermostat (RMT) algorithm,[14] which introduces r thermostatting variables $s_1, s_2, \ldots, s_r$ in such a way that s_1 is directly coupled to the physical variables, s_2 to s_1 and the physical variables, s_3 to s_1, s_2 and the physical variables, and so on. The idea of using different sets of recursive thermostats to different time scale degrees of freedom is related to the idea of *massive thermostatting*.[15] This breaks up the structure of the resulting thermostat and is expected to generate an effective multiscale stochastic heat bath. The following generalized RMT NP Hamiltonian is proposed as

$$\mathcal{H}_{NP}^{RMT} = s_1 \cdots s_r (\mathcal{H}_{Nosé}^{RMT} - \mathcal{H}_0), \tag{8}$$

where

$$\mathcal{H}_{Nosé}^{RMT} = \frac{\tilde{\mathbf{p}}_{\hat{a}}^T \mathbf{m}_{\hat{a}}^{-1} \tilde{\mathbf{p}}_{\hat{a}}}{2s_1^2 \cdots s_r^2} + \frac{\tilde{\mathbf{p}}_{\bar{a}}^T \mathbf{m}_{\bar{a}}^{-1} \tilde{\mathbf{p}}_{\bar{a}}}{2s_2^2 \cdots s_r^2} + \frac{\tilde{\mathbf{p}}_b^T \mathbf{m}_b^{-1} \tilde{\mathbf{p}}_b}{2} + \frac{\pi_r^2}{2\mu_r} + V_{CG}(\boldsymbol{q}, T) + \sum_{k=1}^{r-1} \frac{\pi_k^2}{2\mu_k s_{k+1}^2 \cdots s_r^2} + \hat{g} k_B T \ln s_1 + \sum_{k=2}^{r} \left[(g + k - 1) k_B T \ln s_k + \frac{(1 - s_k)^2}{2C_k} \right]. \tag{9}$$

The sets $\hat{a}$ and $\bar{a}$ represent quantities in the IF and CG9 regions, respectively, $\hat{g}$ and $\bar{g}$ are the numbers of degrees of freedom in those sets, and $g = \hat{g} + \bar{g}$.

Schemes for each of the parts can be constructed by use of a vector field and Hamiltonian splitting.[16] If we denote by ϕ_a, ϕ_b, the numerical integrators associated to thermostatted and unthermostatted degrees of freedom, respectively, then a combined integrator for the whole system can be constructed by the composition:

$$\phi^{\delta t} = \phi_a^{\delta t/2} \phi_b^{\delta t} \phi_a^{\delta t/2}, \tag{10}$$

When ϕ_a and ϕ_b are constructed along the lines of the methods as for PTMD (Ref. 13) they are both volume preserving and time reversible, and the resulting integrator ϕ will share these properties. (Note that the symplectic property of the integrator is sacrificed to maintain scale separation.[13]) For parameters, we have used $r=3$, $\mu_1 = m$, $\mu_2 = 1.2m$, $\mu_3 = 1.5m$, $C_2 = 4.1667\beta$, and $C_3 = 0.003333\beta$.

Now, the long-time sampling problem of Fig. 4 is considered again. The RMT thermostat is applied within the PTMD framework to the IF and CG9 regions of the chain to regulate the temperature to 300 K. The initial temperature of the AR is 600 K. It is clear that RMT equilibrates the chain well with all regions approaching the target temperature within a practical time scale. NP does not achieve this.

Application of RMT to the IF and CG9 regions for the dynamic problem is shown in Fig. 5. It is clearly a great improvement on the NP thermostat. The temperature in the AR is (indirectly) controlled very well by RMT, with practically no phonon reflection. The advantages of RMT are twofold. First, the multiple thermostats can respond to the inherently different frequencies in the different regions. Second, like all Nosé dynamics methods, RMT introduces a feedback control involving average kinetic energy; this control becomes necessarily less sensitive with increasing system size. Modified RMT can respond simultaneously to rapid changes in the small IF and slower changes in the larger CG9 region. The thermostat consequently responds rapidly to the energy entering the IF, absorbing all the high-frequency phonons, and effectively thermostatting the low-frequency CG9 region.

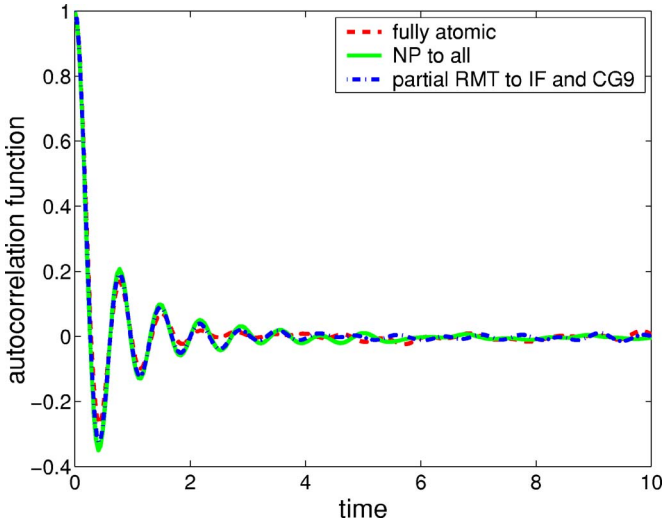

FIG. 6. (Color online) Velocity autocorrelation functions (in terms of momenta) of 20 atoms at the center of the AR for fully NP, PTMD with RMT, and atomistic models: applying strong thermostatting to IF and CG9 regions has not distorted the velocity autocorrelation functions inside the AR.

VI. DISCUSSION AND CONCLUSION

We now turn to the question of recovery of dynamical information from the thermostatted model. We find that PTMD with RMT allows for realistic "dynamics" in two senses of this term.

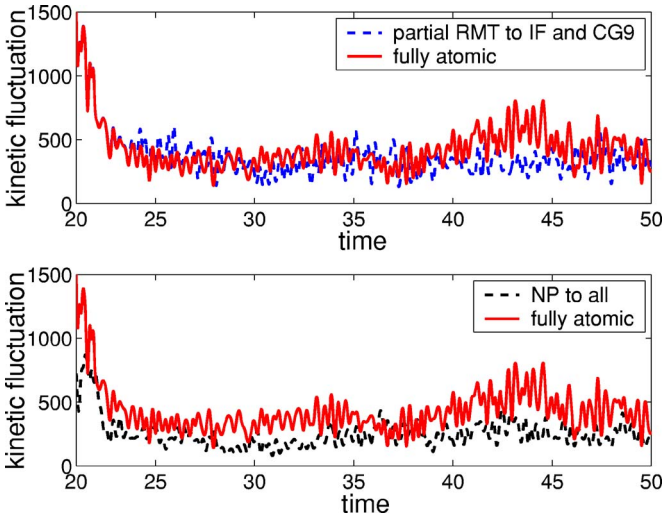

FIG. 7. (Color online) Instantaneous temperature fluctuation of 20 atoms at the center of the AR, for fully (NP) and partially (PTMD) thermostatted simulations, compared with a fully atomistic model.

(i) The long-term (equilibrium) dynamical response is recovered. Figure 6 shows that PTMD with RMT has a very similar velocity autocorrelation function to that of the fully atomistic model (and the NP model) for inner AR atoms.

(ii) The correct transient behavior is observed. Figure 7 shows that NP dynamics gives erroneous kinetic fluctuations (i.e., a lower temperature within the transient time period compared to a fully atomistic simulation), whereas the PTMD with RMT and fully atomistic simulations give matching atomistic trajectories for the inner atoms of the AR within some time interval.

In conclusion, PTMD has been used to provide a coarse-grained heat bath for an atomistic simulation. A single Nosé thermostat cannot adequately thermalize a multiscale chain. RMT provides a hierarchy of successive thermostatting variables to generate a multiscale stochastic heat bath. Application of RMT to an appropriate coarse-grained region has been shown to effectively thermostat highly dynamic simulations without energy trapping and to recover both correct transient fluctuations and equilibrium dynamic response in a 1D model problem.

ACKNOWLEDGMENTS

Financial support for this work from the EPSRC through Grant No. GR/R24104 is gratefully acknowledged by all the authors. The work of B.L. was supported by the Leverhulme Foundation.

[1] S. P. Xiao and T. Belytschko, Comput. Methods Appl. Mech. Eng. **193**, 1645 (2004).
[2] W. K. Liu, E. G. Karpov, S. Zhang, and H. S. Park, Comput. Methods Appl. Mech. Eng. **193**, 1529 (2004).
[3] J. Q. Broughton, F. F. Abraham, N. Bernstein, and E. Kaxiras, Phys. Rev. B **60**, 2391 (1999); R. E. Rudd and J. Q. Broughton, Phys. Status Solidi B **217**, 5893 (2000).
[4] W. K. Liu, E. G. Karpov, and H. S. Park (private communication).
[5] E. B. Tadmor, M. Ortiz, and R. Phillips, Philos. Mag. A **73**, 1529 (1996).
[6] V. B. Shenoy, R. Miller, E. B. Tadmor, R. Phillips, and M. Ortiz, Phys. Rev. Lett. **80**, 742 (1998).
[7] S. Curtaroro and G. Ceder, Phys. Rev. Lett. **88**, 255504 (2002); L. M. Dupuy, E. B. Tadmor, R. E. Miller, and R. Phillips, *ibid.* **95**, 060202 (2005).
[8] R. LeSar, R. Najafabadi, and D. J. Srolovitz, Phys. Rev. Lett. **63**, 624 (1989).
[9] S. Nosé, Mol. Phys. **52**, 522 (1984).
[10] S. D. Bond, B. J. Leimkuhler, and B. B. Laird, J. Comput. Phys. **151**, 114 (1999).
[11] E. Hernandez, J. Chem. Phys. **115**, 10282 (2001).
[12] J. B. Sturgeon and B. B. Laird, J. Chem. Phys. **112**, 3474 (2000).
[13] Z. Jia and B. Leimkuhler, Multiscale Model. Simul. **4**, 563 (2005).
[14] B. J. Leimkuhler and C. R. Sweet, SIAM J. Appl. Dyn. Syst. **4**, 187 (2005).
[15] P. Minary, M. E. Tuckerman, and G. J. Martyna, Phys. Rev. Lett. **93**, 150201 (2004).
[16] B. J. Leimkuhler and S. Reich, *Simulating Hamiltonian Dynamics* (Cambridge University Press, Cambridge, 2005).